Cavity with an embedded polarized film: an adapted spectral approach

2009 J. Phys. A: Math. Theor. 42 165204

(http://iopscience.iop.org/1751-8121/42/16/165204)

IOP PUBLISHING JOURNAL OF PHYSICS A: MATHEMATICAL AND THEORETICAL

J. Phys. A: Math. Theor. **42** (2009) 165204 (18pp) doi:10.1088/1751-8113/42/16/165204

Cavity with an embedded polarized film: an adapted spectral approach

J-G Caputo[1], E V Kazantseva[1], L Loukitch[1] and A I Maimistov[2]

[1] Laboratoire de Mathématiques, INSA de Rouen, BP 8, 76131 Mont-Saint-Aignan cedex, France
[2] Department of Solid State Physics, Moscow Engineering Physics Institute, Kashirskoe sh. 31, Moscow 115409, Russia

E-mail: caputo@insa-rouen.fr, murkamars@hotmail.com and amaimistov@hotmail.com

Received 8 July 2008, in final form 13 February 2009
Published 25 March 2009
Online at stacks.iop.org/JPhysA/42/165204

Abstract
We consider the modes of the electric field of a cavity with an embedded polarized dielectric film. The model consists in the classical Maxwell equations coupled to a Duffing oscillator for the film which we assume infinitely thin. We derive the normal modes of the system and show that they are orthogonal with a special scalar product which we introduce. These modes are well suited to describe the system even for a film of finite thickness. By acting on the film we demonstrate switching from one cavity mode to another. Since the system is linear, little energy is needed for this conversion. Moreover the amplitude equations describe very well this complex system under different perturbations (damping, forcing and nonlinearity) with very few modes. These results are very general and can be applied to different situations like for an atom in a cavity or a Josephson junction in a capacitor and this could be very useful for many nano-physics applications.

PACS numbers: 42.60.Da, 77.55.+f

(Some figures in this article are in colour only in the electronic version)

1. Introduction

There are many reasons to couple an oscillator to a cavity. One example is a laser built using a Fabry–Perot resonator enclosing an active medium which can be modeled as a two-level atom [1, 2]. The cavity can also be used to synchronize oscillators [3] as for an array of Josephson junctions. For window Josephson junctions, used as microwave generators, the Josephson junction collects all the energy in one of the cavity modes [4]. The cavity can also be used as a thermostat to cool the oscillator as described in [5] where an optical cavity is used to

cool an atom. In another example coupling an atom or quantum oscillator to a resonator can significantly change its transport properties [6].

In all the systems described above we have a localized oscillator coupled to a resonator. In addition the size of the oscillator can often be neglected. This situation can be represented by a thin film model [7, 8]. Such a thin film model was generalized by taking into account the local field effects (dipole–dipole interaction) [9–11]. Intrinsic optical bistability is the main result of this generalization. Thin films containing three-level atoms [12], two-photon resonant atoms [13, 14], inhomogeneously broadened two-level [15] atoms and two-level atoms with permanent dipole [16] represent the different generalizations of the model. The coherent responses of resonant atoms of a thin film to short optical pulse excitation were considered in [15]. It was shown that for a certain intensity the incident pulse generates sharp spikes in the transmitted radiation. Photon echo in the form of multiple responses to a double or triple pulse excitation was predicted also in this paper. The coherent reflection from a thin film as superradiation was studied in [17–19].

Recently we used the thin film model to describe switching phenomena in ferroelectrics [21]. The behavior of the new artificial materials—metamaterials—under the action of electromagnetic pulses could also be described by this model [22]. As we see, the thin film model is extremely fruitful, the investigation of the behavior of the thin film embedded inside the cavity is a very attractive problem. When the model of a thin film is explored, the problem of the matter–field interaction reduces to that of an electromagnetic cavity with an embedded (linear or nonlinear) oscillator. Frequently the nonlinear problem is analyzed using coupled mode equations. In this approach the relevant values are the amplitudes of each of the linear modes. The nonlinear partial differential equation of motion is reduced to a system of coupled ordinary differential equations for the amplitudes of the linear modes. A suitable choice of the linear modes allows us to get an effective description of the original problem.

We consider here this simplest and most general situation, first for small energy for which the problem is linear. Similar models have been recently considered for cavity electrodynamics by Meystre *et al* [23, 24] and Domokos *et al* [25]. One can also consult [26, 27] for the full quantum treatment of a leaky laser cavity. In these studies, the internal structure of the atoms interacting with the cavity is eliminated and the coupling of the field at the atoms is described by reflection and transmission coefficients. Then the atom is 'slaved' to the electromagnetic field and the coupling is asymmetric. In our complementary approach, we keep both the field e and the medium variable q thereby allowing a symmetric coupling. We will consider the normal modes of the film–cavity coupled system. These are solutions of a non-standard boundary value problem. These two-component (e, q) modes are necessary to describe the evolution of the system (10). We show in the appendix that standard Fourier modes or other eigenmodes do not describe the frequency dependent interaction. These adapted eigenmodes are orthogonal with respect to a special scalar product which we introduce. Using these modes we can define simply the state of the system. We will show that one can get mode conversion by acting on the film sub-system. This mechanism can be applied to the different systems described above. In the nonlinear case, for medium amplitudes, we show that a few modes are sufficient to describe the evolution of the system. Although our study is classical, it could be useful to compare it with the formalism of cavity quantum electrodynamics (CQED) [20].

After introducing the model in section 2, we consider the linear limit in section 3 and derive the normal modes of the system. The special scalar product is derived in section 4. In sections 5 and 6 we use the normal modes to define the state of the (linear) system and show mode conversion when driving and damping the film. We also describe the general nonlinear case and we conclude in section 7.

2. The thin film model

We consider a one-dimensional model of the electromagnetic radiation interacting with a polarized dielectric film inside a cavity. The film is placed at the distance x_a inside the cavity having the length l. The Lagrangian density for the electromagnetic field, the film medium and their coupling is the following [21]:

$$\mathcal{L} = \frac{a_t^2}{2} - \frac{a_x^2}{2} + \delta\left(x - x_a\right)\left(\frac{q_t^2}{2} - m\frac{q^2}{2} - \frac{q^4}{4} - \alpha q a_t\right). \tag{1}$$

Here a is the analog of vector potential and q is the medium polarization, α is a coupling constant. The last term in the Lagrangian describes the coupling between a and q. The dielectric medium can be ferroelectric ($m = -1$) with two polarizations or paraelectric $m = 1$. The Hamiltonian of the system is

$$\mathcal{H} = a_t \frac{\partial \mathcal{L}}{\partial a_t} + q_t \frac{\partial \mathcal{L}}{\partial q_t} - \mathcal{L}, \tag{2}$$

which gives

$$\mathcal{H} = \frac{a_t^2}{2} + \frac{a_x^2}{2} + \delta\left(x - x_a\right)\left(\frac{q_t^2}{2} + m\frac{q^2}{2} + \frac{q^4}{4}\right). \tag{3}$$

Note that the coupling is absent from $\mathcal{H}$. It appears instead in the momentum associated with a, $p_a \equiv \frac{\partial \mathcal{L}}{\partial a_t} = a_t - \delta\left(x - x_a\right)\alpha q$.

The variation of the action functional yields the Euler–Lagrange equations for a and q

$$\frac{\partial \mathcal{L}}{\partial a} = \frac{\mathrm{d}}{\mathrm{d}t}\frac{\partial \mathcal{L}}{\partial a_t} + \frac{\mathrm{d}}{\mathrm{d}x}\frac{\partial \mathcal{L}}{\partial a_x}, \tag{4}$$

$$\frac{\partial \mathcal{L}}{\partial q} = \frac{\mathrm{d}}{\mathrm{d}t}\frac{\partial \mathcal{L}}{\partial q_t} + \frac{\mathrm{d}}{\mathrm{d}x}\frac{\partial \mathcal{L}}{\partial q_x}, \tag{5}$$

which reduce to

$$a_{tt} - a_{xx} = \alpha\delta\left(x - x_a\right) q_t, \tag{6}$$

$$q_{tt} + mq + q^3 = -\alpha a_t. \tag{7}$$

The equations for the electric field $e = -a_t$ and medium variable can then be obtained

$$e_{tt} - e_{xx} = -\alpha\delta(x - x_a) q_{tt}, \tag{8}$$

$$q_{tt} + mq + q^3 = \alpha e(x_a), \tag{9}$$

where the coupling between the fields e and q only occurs in the medium at $x = x_a$.

In a recent article [21], we considered with this model the interaction of a thin dielectric film with an electromagnetic pulse. We studied both the case of a ferroelectric and paraelectric film. For the ferroelectric film we showed that the polarization can be switched by an incoming pulse and studied this phenomenon. Here we will assume that the film is embedded in a cavity and we will study how cavity modes can be controlled by the film. Specifically we will assume Dirichlet boundary conditions for the field.

For small amplitudes of the field, it is natural to neglect the nonlinear response of the film. Note however that the ferroelectric film and paraelectric film have different natural frequencies corresponding to different stationary points. For the paraelectric case, there is only one fixed point $q = 0$ while for the ferroelectric case there are three fixed points, the unstable one $q = 0$

and the two stable ones $q = \pm 1$ corresponding to two opposite signs of the polarization. It is then natural to introduce the natural frequency of the oscillator $\omega_0^2 = m$ for the paraelectric case and $\omega_0^2 = m + 3q_0^2$ for the ferroelectric case. We therefore consider below the general linear problem of a harmonic oscillator of frequency ω_0 embedded in a cavity.

3. The linear limit: normal modes

The linear problem is

$$e_{tt} - e_{xx} = -\alpha\delta\,(x - x_a)\,q_{tt}, \tag{10}$$

$$q_{tt} + \omega_0^2 q = \alpha e(x_a). \tag{11}$$

Note that we have a Dirac delta function in the first equation so that the solution will not have a second derivative at $x = x_a$. In this case, one can write the solution using standard sine Fourier modes. However these are not adapted to describe the evolution because the projection of the operator gives wrong results [28]. Then we need to define new normal modes. For this one first separates time and space and then looks for solutions in the form

$$e(x,t) = E(x)\,\mathrm{e}^{\mathrm{i}\omega t}, \qquad q(x,t) = Q(x)\,\mathrm{e}^{\mathrm{i}\omega t},$$

so that the system (10) becomes

$$E''(x) + \omega^2 E(x) = -\alpha\omega^2 Q\delta(x - x_a), \qquad Q = \frac{\alpha E(x_a)}{\omega_0^2 - \omega^2}. \tag{12}$$

As expected from the general theory of linear operators [29] the system will exhibit eigenfrequencies and eigenmodes (normal modes). Combining these two equations, we obtain the final boundary value problem for E

$$E''(x) + \omega^2\left(1 + \frac{\alpha^2\delta(x - x_a)}{\omega_0^2 - \omega^2}\right)E(x) = 0, \tag{13}$$

with the boundary conditions $E(0) = E(l) = 0$.

To obtain the solution, note that except for $x = x_a$

$$E''(x) + \omega^2 E(x) = 0.$$

Using this remark and the boundary conditions we get the left and right solutions

$$E(x) = \begin{cases} A\sin\omega x, & x < x_a, \\ B\sin\omega(l - x), & x > x_a, \end{cases} \tag{14}$$

where A and B are constants. To connect the left and right solutions we use the continuity of $E(x)$ as well as of e at $x = x_a$. The second relation needed is the jump condition for E' obtained by integrating (13) over a small interval centered on x_a. When the size of the interval goes to zero we get

$$[E']_{x_a^-}^{x_a^+} = -\frac{\alpha^2\omega^2}{\omega_0^2 - \omega^2}E(x_a). \tag{15}$$

At $x = x_a$ the continuity of E and jump condition (15) give the following relations:

$$A\sin\omega x_a - B\sin\omega(l - x_a) = 0, \tag{16}$$

$$A\left(\frac{\alpha^2\omega}{\omega_0^2 - \omega^2}\sin\omega x_a - \cos\omega x_a\right) - B\cos\omega(l - x_a) = 0. \tag{17}$$

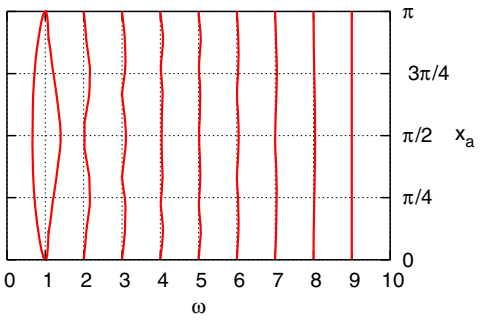

Figure 1. Eigenvalues (zeros of the dispersion relation (18)) as a function of the position of the film x_a. The parameters are $l = \pi$, $\alpha = 1$ and $\omega_0 = 1$.

For this homogeneous system to have a nonzero solution, the determinant must be zero and this gives the dispersion relation

$$\sin \omega l = \alpha^2 \frac{\omega}{\omega_0^2 - \omega^2} \sin \omega x_a \sin \omega (l - x_a), \tag{18}$$

which determines the allowed frequencies ω of the system.

As can be expected from the general theory [29], we have an infinite countable set of allowed frequencies. Note that in the absence of coupling to the film $\alpha = 0$, we get the standard Fourier modes $\omega_n = n\pi/l$. For small α the shift in frequency is small because the right-hand side is proportional to α^2. These eigenfrequencies can be computed using bisection for example.

To summarize, the eigenvalues and eigenvectors (up to a multiplicative constant) of the boundary value problem (12) are

$$\left\{ \omega_i, \mathbf{V}_i = \begin{pmatrix} E_i(x) \\ Q_i \end{pmatrix} \right\}, \tag{19}$$

where

$$E_i(x) = \begin{cases} \sin \omega_i x, & x < x_a, \\ \dfrac{\sin \omega_i x_a}{\sin \omega_i (l - x_a)} \sin \omega_i (l - x), & x > x_a, \end{cases} \qquad Q_i = \frac{\alpha E_i(x_a)}{\omega_0^2 - \omega_i^2}, \tag{20}$$

and ω_i satisfies (18).

Note that an equation similar to (13) was obtained in the theory of a 1D waveguide with a perfect mirror at one end and a two-level atom at the other end [30]. Contrary to our case, this is not an eigenvalue problem because the system is open on one side. From another point of view, the system cavity/film (10) was considered for $\omega_0 = 0$ by Bocchieri *et al* [31] in the context of statistical mechanics. Their main result was that there was always energy exchange between the film and the cavity so that equipartition could not be reached. Indeed, this can be seen by examining the normal modes (20) which couple E_i and Q_i. Only for special symmetries (film at the center of the cavity . . .) and special frequencies do we get $Q_i = 0$.

3.1. Influence of the film parameters on the dispersion relation

We now study the dispersion relation in more detail. In figure 1 we plot the solutions of (18) as a function of the film position for $\omega_0 = 1$ and $\alpha = 1$. Note how the systems generate two eigenvalues in place of the frequency $\omega_0 = 1$. For large frequencies $\omega \gg \omega_0$ we recover

the standard Fourier cavity modes $\omega_n = n\pi/l$. The eigenmodes for the particular case of a centered film shown in figure 1 contain the even Fourier modes. These correspond to $Q_i = 0$ because their derivative is continuous at x_a. This will have important practical consequences.

Because of the film, the eigenfrequencies of the system film/cavity differ from the usual Fourier cavity modes $\omega_n = n\pi/l$. They are shifted if $\omega_n \neq \omega_0$ and disappear if $\omega_n = \omega_0$. Let us compute this shift in the limit of small α using perturbation theory. To simplify the analysis, we assume $l = \pi$ so that $\omega_n = n\pi/l = n$. We search the frequency ω using the expansion

$$\omega = n + \alpha^2\omega_1 + \cdots,$$

with $\omega_1 \ll 1$ and n are the usual sine Fourier modes of the cavity. We have the following relations:

$$\begin{aligned}
&\sin \omega l = (-1)^n \alpha^2 \omega_1 \pi + O(\alpha^4),\\
&\sin \omega x_a = \sin n x_a + \alpha^2 \omega_1 x_a \cos n x_a + O(\alpha^4),\\
&\sin \omega (l - x_a) = \sin n(l - x_a) + \alpha^2 \omega_1 (l - x_a) \cos n(l - x_a) + O(\alpha^4).
\end{aligned}$$

Plugging these relations into (18) we have, up to $O(\alpha^4)$

$$(-1)^n \omega_1 = \frac{n}{\pi\left(\omega_0^2 - n^2\right)} \sin n x_a \sin n(l - x_a). \tag{21}$$

Assuming that $\alpha^2 < 1$ we get the simplified expression

$$\omega = n - \alpha^2 (-1)^n \frac{n}{\pi} \frac{1}{\omega_0^2 - n^2} \sin n x_a \sin n(l - x_a) + O(\alpha^4). \tag{22}$$

Due to the presence of the film the cavity modes close to the film mode are blueshifted if the frequency of the cavity mode is above the oscillator eigenfrequency and redshifted for lower cavity mode frequencies.

When $\omega_0^2 = n_0^2$ where n_0 is an integer, the oscillator frequency coincides with the cavity mode. In this case the eigenfrequency of the combined system splits away from n_0. This is a general property of coupled oscillators. The splitting can be calculated for small α by assuming

$$\omega = \omega_0 + \omega_1,$$

where $|\omega_1| \ll \omega_0$.

Plugging this expression into the dispersion relation and collecting the terms, we obtain the second-degree equation

$$A{\omega_1}^2 + B\omega_1 + C = 0,$$

where

$$A = 4\pi n + \alpha^2((\pi - 2x_a)\sin 2nx_a - (\cos 2nx_a - 1)n/2), \tag{23}$$

$$B = \alpha^2(n(\pi - 2x_a)\sin 2nx_a + \cos 2nx_a - 1), \tag{24}$$

$$C = \alpha^2 n(\cos 2nx_a - 1). \tag{25}$$

The two branches of the resonant frequency are then given by

$$\omega_1 = \frac{-B \pm \sqrt{B^2 - 4AC}}{2A}.$$

As an example, consider the case of figure 1 corresponding to $l = \pi$ and a film placed in the center of the cavity $x_a = 0.5l$. Then $\cos\omega(l - 2x_a) = 1$ and $\cos \omega l \approx (-1)^{n_0}\left(1 - \omega_1^2/2\right)$.

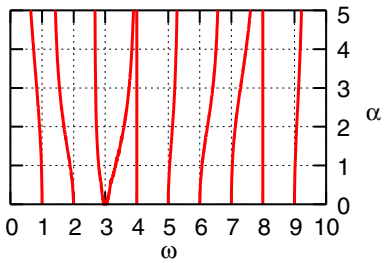

Figure 2. Plot of the first 10 eigenfrequencies as a function of the coupling parameter α for an off-centered film $x_a = l/4 = \pi/4$ whose frequency is $\omega_0 = 3$.

Then the splitting is given by

$$4\pi n_0 \omega_1^2 = \alpha^2 (n_0 + \omega_1)\big(1 - \omega_1^2/2\big)(1 - (-1)^{n_0}), \tag{26}$$

so that $\omega_1 = 0$ for even resonant frequency n_0 and there is no shift from the resonance in this case. For the odd n_0 we obtain the quadratic equation for the frequency detunings ω_1 from the resonance

$$\omega_1^2 - \frac{\alpha^2 \omega_1}{n_0(2\pi + \alpha^2/2)} - \frac{\alpha^2}{2\pi + \alpha^2/2} = 0, \tag{27}$$

$$\omega_1 = \frac{\alpha^2}{2n(2\pi + \alpha^2/2)} \left(1 \pm \sqrt{1 + \frac{4{n_0}^2(2\pi + \alpha^2/2)}{\alpha^2}} \right). \tag{28}$$

When α increases, the influence of the film grows and the eigenfrequencies become very different from the Fourier cavity modes. In fact when $\alpha \gg 1$, the dominating term in the dispersion relation is the right-hand side and we obtain

$$\sin \omega x_a = 0, \qquad \text{or} \qquad \sin \omega (l - x_a) = 0,$$

so that

$$\omega_n = \frac{n\pi}{x_a}, \qquad \text{or} \qquad \omega_n = \frac{n\pi}{l - x_a}. \tag{29}$$

This corresponds to oscillations in the left or right cavities. Figure 2 shows the first 10 eigenfrequencies as a function of the coupling parameter α for a cavity of length $l = \pi$ and an off-centered film $x_a = l/4$ whose frequency $\omega_0 = 3$. Note the splitting for $\omega = 3$. As α increases, the eigenfrequencies tend to those given by (29), i.e. $\omega_n = 4n$ or $\omega_n = 4n/3$.

4. Orthogonality of the normal modes

Using the vector notation $\mathbf{V}$ defined above, the original linear system (10) can be formally written as

$$\big(\partial_t^2 + \mathbf{L}\big)\mathbf{V} = 0, \tag{30}$$

where the operator $\mathbf{L}$ is

$$\mathbf{L} = -\partial_x^2 \begin{pmatrix} 1 & 0 \\ 0 & 0 \end{pmatrix} + \begin{pmatrix} \alpha^2 \delta(x - x_a) & -\alpha \omega_0^2 \delta(x - x_a) \\ -\alpha \int \delta(x - x_a) & \omega_0^2 \end{pmatrix}. \tag{31}$$

The eigenfrequencies and eigenvectors ω_i, $\mathbf{V}_i$ are such that

$$L\mathbf{V}_i = \omega_i^2 \mathbf{V}_i. \tag{32}$$

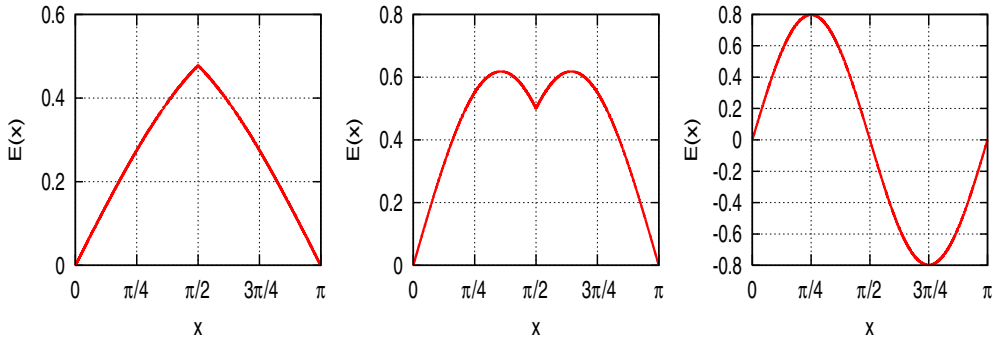

Figure 3. Plot of the E component of the normalized first, second and third eigenmodes. The film is in the middle of the cavity $x_a = \pi/2$. The other parameters are the same as in figure 1.

The boundary value problem (13) is not a standard Sturm–Liouville problem because the potential depends on the eigenvalue. Therefore one needs to define a particular scalar product so that the normal modes $\mathbf{V}_i$ defined previously are orthogonal. This is crucial if we want to use these modes as vectors on which we can project the state of the linear system (10) and therefore obtain a simplified description.

To define this scalar product consider equation (12) with two solutions

$$E_j''(x) + \omega_j^2 E_j(x) + \alpha\omega_j^2 Q_j \delta(x - x_a) = 0, \tag{33}$$

$$E_i''(x) + \omega_i^2 E_i(x) + \alpha\omega_i^2 Q_i \delta(x - x_a) = 0. \tag{34}$$

To show orthogonality the equation for E_i is multiplied by E_j and vice versa. Subtracting the resulting equations one obtains

$$E_i E_j'' - E_j E_i'' + \left(\omega_j^2 - \omega_i^2\right) E_i E_j + \alpha\delta(x - x_a)\left(E_i\omega_j^2 Q_j - E_j\omega_i^2 Q_i\right) = 0. \tag{35}$$

After integration the resulting equation on the domain $[0; l]$ the first two terms drop out because of the boundary conditions. Substituting E_i, E_j from (20) in the last term leads to the following:

$$\left(\omega_j^2 - \omega_i^2\right)\left[\int_0^l E_i E_j \,\mathrm{d}x + \omega_0^2 Q_i Q_j\right] = 0. \tag{36}$$

This shows that for $\omega_i \neq \omega_j$ the term in the brackets should be zero. The scalar product is then defined as

$$\langle \mathbf{V}_i; \mathbf{V}_j \rangle \equiv \int_0^l E_i E_j \,\mathrm{d}x + \omega_0^2 Q_i Q_j. \tag{37}$$

Relation (37) establishes a strictly positive linear form, so it is a scalar product.

Equation (36) shows the orthogonality of the eigenvectors V_i for the scalar product defined by equation (37). Now it is possible to choose A_i such that the vectors are normalized

$$\langle \mathbf{V}_i; \mathbf{V}_i \rangle = 1.$$

For this we compute $\langle \mathbf{V}_i; \mathbf{V}_i \rangle$, set it equal to 1 and this gives the value of A_i.

The normalized eigenvalues are plotted in figure 3 together with the associated Q_i in figure 4 for a film placed in the center of a cavity of length $l = \pi$. Note the clear break in the derivative at x_a. The orthogonality of the modes $(\mathbf{V}_i, \mathbf{V}_j)$ comes from the compensation of the integral of $E_i E_j$ by the product $Q_i Q_j$.

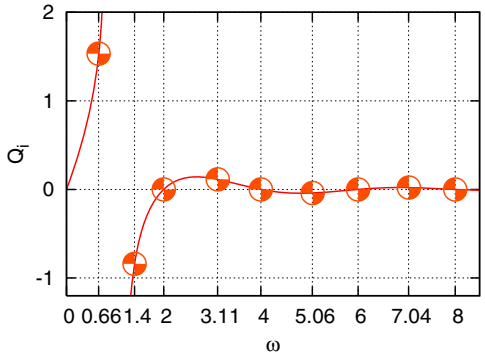

Figure 4. Plot of the Q_i components of the normalized eigenmodes as a function of ω for $x_a = \pi/2, l = \pi$. The eigenvalues are indicated by the vertical lines.

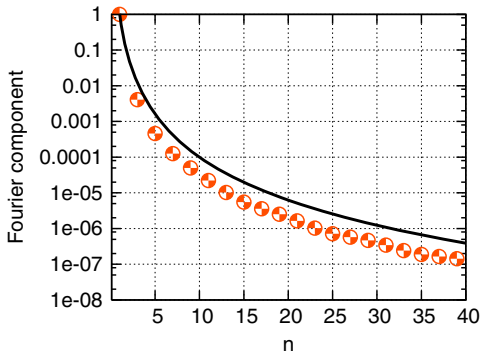

Figure 5. Plot of the squares of the Fourier sine coefficients of the E component of the first normal mode in the log-linear scale. The function $1/n^4$ is plotted as a continuous line.

These modes are specially adapted to describe the coupled system film/cavity. Many standard sine Fourier modes are necessary to get a good approximation of the first normal mode. This is seen in figure 5 which shows the amplitude square of the sine Fourier coefficients of the first normal mode. Note the typical $1/n^4$ decay due to the fact that the second derivative of E is singular at $x = x_a$ [32].

When the film is shifted to one side of the cavity, the modes become asymmetric as shown in figure 6. Again the break in the derivative is clearly apparent. Here standard Fourier modes only appear for $n = 4, 8, \ldots$. The Q_i decay very quickly to 0 as shown in figure 7.

5. Cavity mode transfer using an active film

The normal modes defined in the previous section define a basis to describe the state of the combined system cavity/film. We now show that it is possible by acting on the film to switch the cavity from one mode to another neighboring mode. This feature is impossible for a single linear system. It is possible here because of the combination of the two linear subsystems: the cavity and the film.

In order to describe analytically this process, we introduce the forcing of the film as $f(q, q_t, t)$ and write the system as

$$e_{tt} - e_{xx} = -\alpha\delta\,(x - x_a)\,q_{tt}, \tag{38}$$

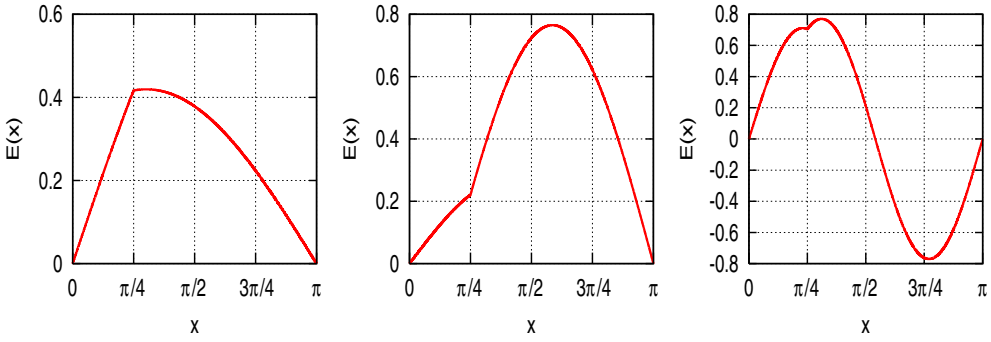

Figure 6. Plot of the E component of the normalized first, second and third eigenmodes. The film is shifted to the left of the cavity $x_a = \pi/4$. The other parameters are the same as in figure 1.

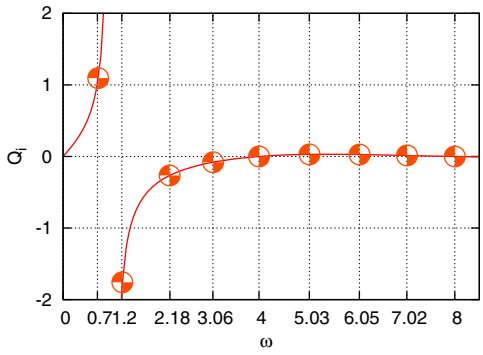

Figure 7. Plot of the Q_i components of the normalized eigenmodes as a function of ω for $x_a = l/4, l = \pi$. The eigenvalues are indicated by the vertical lines.

$$q_{tt} + \omega_0^2 q = \alpha e(x_a) + f(q_t, t). \tag{39}$$

Using the vector notation $\mathbf{V}$ of the previous section, this system can be formally written as

$$\left(\partial_t^2 + \mathbf{L}\right)\mathbf{V} = \mathbf{F}, \tag{40}$$

where the operator $\mathbf{L}$ is given by (31) and the forcing is

$$\mathbf{F} = \begin{pmatrix} -\alpha\delta(x - x_a) f \\ f \end{pmatrix}. \tag{41}$$

For this linear system, it is natural to expand the state vector $\mathbf{V}$ in terms of the (normalized) normal modes

$$\mathbf{V} = \begin{pmatrix} e \\ q \end{pmatrix} = \sum_i \alpha_i(t)\mathbf{V}_i, \tag{42}$$

where the normal modes $\mathbf{V}_i$ verify the relation $\mathbf{L}\mathbf{V}_i = \omega_i^2 \mathbf{V}_i$. Plugging (42) into the equation (40) and projecting over each normal mode we get

$$\ddot{\alpha}_i + \alpha_i \omega_i^2 = \langle \mathbf{V}_i \mathbf{F} \rangle, \qquad i = 1, 2, \ldots, \tag{43}$$

where the scalar product

$$\langle \mathbf{V}_i \mathbf{F} \rangle = \int_0^l E_i(-\alpha f \delta(x - x_a))\,\mathrm{d}x + \omega_0^2 Q_i f = \omega_i^2 Q_i f. \tag{44}$$

To be specific, we now assume that f consists in a damping and forcing term

$$f(t) = -\gamma(t) q_t + I(t). \tag{45}$$

This is a natural choice for the theory since we are dealing with linear oscillators. Note also that such a pulse could be easily prepared in an experiment. Recalling the linear combination (42) $q_t = \sum_n \dot{\alpha}_n Q_n$ we get the final expression of the scalar product (44)

$$\langle \mathbf{V}_i \mathbf{F} \rangle = -\gamma(t)\omega_i^2 Q_i \sum_n \dot{\alpha}_n Q_n + \omega_i^2 Q_i I(t). \tag{46}$$

To illustrate this, consider just two modes in expansion (42). The system describing the evolution of the mode amplitudes is then

$$\ddot{\alpha}_1 + \alpha_1 \omega_1^2 = -\gamma(t)\omega_1^2 Q_1(\dot{\alpha}_1 Q_1 + \dot{\alpha}_2 Q_2) + \omega_1^2 Q_1 I(t), \tag{47}$$

$$\ddot{\alpha}_2 + \alpha_2 \omega_2^2 = -\gamma(t)\omega_2^2 Q_2(\dot{\alpha}_1 Q_1 + \dot{\alpha}_2 Q_2) + \omega_2^2 Q_2 I(t). \tag{48}$$

Note that only using the normal modes (19) and (20) and the scalar product (37) does one obtain a consistent modal description of the system. Using for example the standard Sturm–Liouville modes associated with a linear impurity placed at $x = x_a$ leads to an inconsistency. This important fact is shown in appendix A.

Also remark that for $l = \pi$, $a = l/2$, the normal modes include the even (standard) sine Fourier modes. These however are decoupled from all the other modes because for them $Q_i = 0$ so the right-hand side of the amplitude equation (47) is zero.

6. Numerical simulations

To test these ideas, we have undertaken numerical simulations of equations (10) using the method of lines, where the spatial operator is integrated over reference intervals (finite volume method). The time evolution is then done using an ordinary differential equation solver. The algorithm is described in appendix B.

6.1. Linear regime

We introduce a characteristic forcing time function

$$g(t) = \frac{1}{2}\left[\tanh\left(\frac{t - t_1}{w_t}\right) - \tanh\left(\frac{t - t_2}{w_t}\right)\right], \tag{49}$$

and assume that the damping and forcing are

$$\gamma(t) = g(t)\gamma_0, \qquad I(t) = g(t)\beta \sin(\omega t + \phi), \tag{50}$$

where γ_0, β, ω and ϕ are parameters. We consider the case of a centered film $x_a = l/2 = \pi/2$. For all the runs presented, we chose $\gamma_0 = 0.1$, $\beta = 0.2$, $\phi = 0$ and a time interval of forcing $[t_1, t_2] = [50, 100]$ with $w_t = 1$. Unless otherwise specified, the initial state of the system is the first normal mode.

As a first step, we validate our mode amplitude differential equations (47) by comparing their solution with the mode amplitudes obtained by projecting the solution of the partial differential equation (10) onto the normal modes $\mathbf{V}_i$ given by (19) and (20). The integrals are

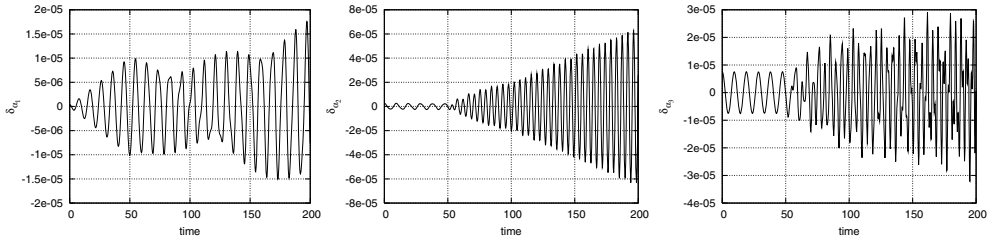

Figure 8. Time evolution of the absolute difference $|\alpha_i(t) - \alpha_i'(t)|$, $i = 1, 2, 3$ (from left to right) between the solution of the amplitude equations (47) and the coefficients obtained by projecting the solution of the full partial differential equation (10). The system has been forced at frequency $\omega = 1.4 \approx \omega_2$ during the time $50 < t < 100$.

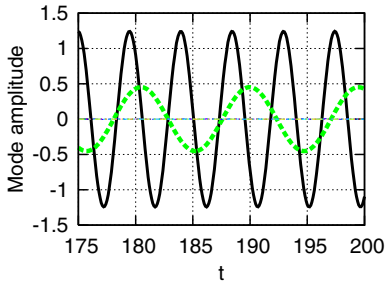

Figure 9. Plot of $\alpha_i(t)$ for $i = 1$ (dashed line, green online) and $i = 2$ (continuous line) after having forced the system at frequency $\omega = 1.4 \approx \omega_2$. The system is started in the mode 1 only, $\alpha_1 = 1$.

calculated using the trapeze method using 800 mesh points. Figure 8 shows the absolute error in log scale as a function of time for the first three modes (except even Fourier modes). The difference is consistent with the error made in the trapeze integration method $O(h^2)$. Note that for $i = 2$ the difference increases during the forcing. This is due to the appearance of new modes as shown below. The agreement is excellent and the error of about 10^{-5} is essentially the error in the trapeze method $h^2 = (\pi/800)^2 \approx 10^{-5}$. If only the first three modes are used in the amplitude equations, the error is still very small. In many other cases, we compared the solution of the full problem (10) with that given by the amplitude equations (47) and always found errors of about 10^{-5}. This shows that these simple amplitude equations are a precise way to describe the complex system film/cavity.

After this validation, we examine the role of the forcing frequency and show that we can transfer energy from one cavity mode to another by acting on the film via the forcing and damping (50). The value of the forcing frequency is essential as shown in the following figures. First we chose $\omega = 1.4 \approx \omega_2$ so that we are forcing the system to resonate in the second normal mode. The energy transfer is then efficient and after a short time of forcing we find the system in the normal mode 2 with very little left of the normal mode 1. This is shown in figure 9 where we plot the initial mode as a dashed line and the newly generated mode as a continuous line. This notation will be used throughout this section. We now change the forcing frequency to $\omega = 1$ and retain otherwise the same protocol. In this case we do not have a resonance of the system and it responds by generating components on the neighboring normal modes. When forcing the system on the sine Fourier mode $\omega_3 = 2$ for which $Q_3 = 0$

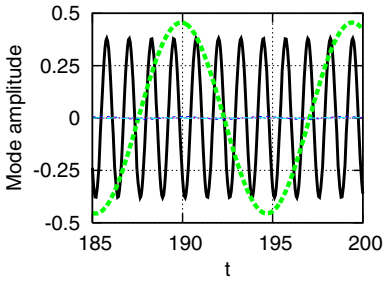

Figure 10. Plot of $\alpha_i(t)$ for $i = 6$ (continuous line) and $i = 1$ (dashed line) after having forced the system at frequency $\omega = 5 \approx \omega_6 = 5.06....$ The system is started in the mode 1 only, $\alpha_1 = 1$.

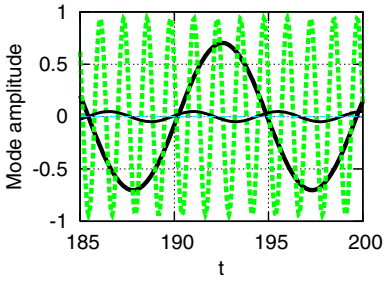

Figure 11. Plot of $\alpha_i(t)$ for $i = 6$ (dashed line) and $i = 1, 2$ (continuous line) after having forced the system at frequency $\omega \approx \omega_1 = 0.66$. The mode 3 is also present as shown by the short dashed line (blue line). The system is started in the mode 6 only, $\alpha_6 = 1$.

no energy is fed into this mode as expected from the amplitude equations (47). The system responds on the first, second and fourth normal modes. We have forced the system at frequency $\omega = 5$ and obtained conversion from mode 1 to mode 6. This is shown in figure 10. If we choose ω closer to ω_6 the transfer is even better so that the amplitude of the mode 6 is larger. Note that it is also possible to obtain down conversion of modes. For example starting with mode 6 and forcing at a frequency $\omega = 0.66 \approx \omega_1$ we obtain the mode 1 and a little of mode 2. This is shown in figure 11. The value of Q_i determines the efficiency of conversion to or from the mode i. For example with a cavity of length $l = \pi$ and a film placed at $a = l/2$, we find $Q_1 = 1.8$ and $Q_6 = -0.15$. We can then state that in general, conversion from modes close to ω_0 to normal modes far from ω_0 is more efficient than the converse. This is because in the amplitude equations (47) the damping of α_i is proportional to Q_i^2 while the amplification term is proportional to Q_i. So a mode close to resonance with a large Q_i is damped more than another normal mode with a smaller Q_j. This is shown in figures 10 and 11.

Finally let us comment on the influence of the damping, forcing time and frequency on the mode transfer. The main effect of the damping is to eliminate the original starting mode whose evolution is given by an exponentially damped oscillation [33]. The forced mode appears through linear resonance, its amplitude increases linearly during the forcing time and its final amplitude does not depend strongly on the damping. As an example consider an increase of the damping from 0.1 to 0.5 for the case shown in figure 10. Then the amplitude of the first mode is reduced from 0.4 to about 0.02 and the amplitude of the sixth mode remains practically unchanged at about 0.4. Last, because this is a linear resonance it is important to be close to the resonant frequency in order to excite the corresponding mode. In practice, the window of resonance is given by the damping term in (47), $\delta\omega = \gamma\omega_i^2 Q_i^2$. For the case of

figure 10, we get $\delta\omega = 0.125$ for a damping $\gamma_0 = 0.5$. In fact, taking $\omega = 4.5$ instead of 5 will only yield an amplitude of 0.1 for the amplitude of the sixth mode.

To summarize we have shown that this linear system can convert energy from one normal mode to another. This was thought impossible for a linear system because of the orthogonality of the normal modes. Here because we act on the sub-system we are able to do this transfer. Another important result is the excellent agreement between the solution of the amplitude equations and the solutions of the initial problem. This simple method could then be used in practice to solve the singular partial differential equation (10).

6.2. Nonlinear regime

Another way to convert energy from one mode to another is through nonlinearity. A well-known example is the famous study of Fermi, Pasta and Ulam (see for example the entry in [34]) showing energy recurrence between Fourier modes in a chain of anharmonic oscillators. Now we consider the film to follow a law with a cubic nonlinearity and take out the driving and damping terms.

The film equation now incorporates a cubic nonlinearity so that the composite cavity/film is described by system (8). The cubic term can be treated as in the previous section and incorporated into the F term of equation (40). The scalar product is

$$\langle \mathbf{V}_i \mathbf{F} \rangle = \omega_i^2 Q_i q^3 = \omega_i^2 Q_i \left(\sum_n \alpha_n Q_n \right)^3 . \tag{51}$$

Then the amplitude equations are

$$\ddot{\alpha}_1 + \alpha_1 \omega_1^2 = \omega_1^2 Q_1 \left(\sum_n \alpha_n Q_n \right)^3 , \tag{52}$$

$$\ddot{\alpha}_2 + \alpha_2 \omega_2^2 = \omega_2^2 Q_2 \left(\sum_n \alpha_n Q_n \right)^3 . \tag{53}$$

$\ldots$

If there is in addition forcing and damping on the system, one needs to add to the right-hand side of (52) the terms on the right-hand side of (47).

As the amplitude of the film polarization q increases, one expects that higher and lower frequency normal modes will be excited. This coupling to the other modes is clear from the right-hand side of the amplitude equations (52). Of course one should not increase too much the amplitude of the forcing because then the wavelength of the cavity modes would reduce and become comparable with the film thickness. Then approximating the film by a Dirac distribution would not make sense.

We start the system in the first normal mode with zero amplitude and a positive velocity and let it evolve from 0. This procedure is chosen so as not to create a shock in the system with the nonlinearity. For small velocities, there is little transfer from the first to the second and third modes. Again the sine Fourier modes do not play any role because for them $Q_i = 0$. Increasing the initial velocity increases the transfer of energy to the higher modes. For a velocity of 0.5, figure 12 shows the evolution of $\alpha_i, i = 1 - 4$ as a function of time for both the full system (8) and the amplitude equations (52). As expected the nonlinearity generates higher frequencies. Note the excellent agreement between the solution of the partial differential equation system and the amplitude equations. This holds even for such large velocities as 2.

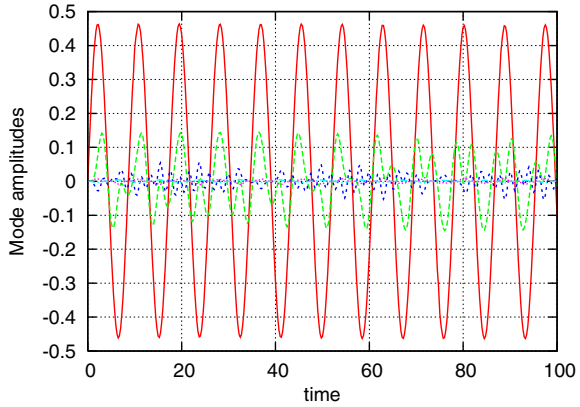

Figure 12. Plot of $\alpha_i(t)$ for $i = 1$ (continuous line), $i = 2$ (long dash), $i = 3$ (short dash) for a system with cubic nonlinearity. The results from the amplitude equations (52) with eight modes are also plotted and they superpose exactly. The initial velocity is 0.5. The system is started in the mode 1 only.

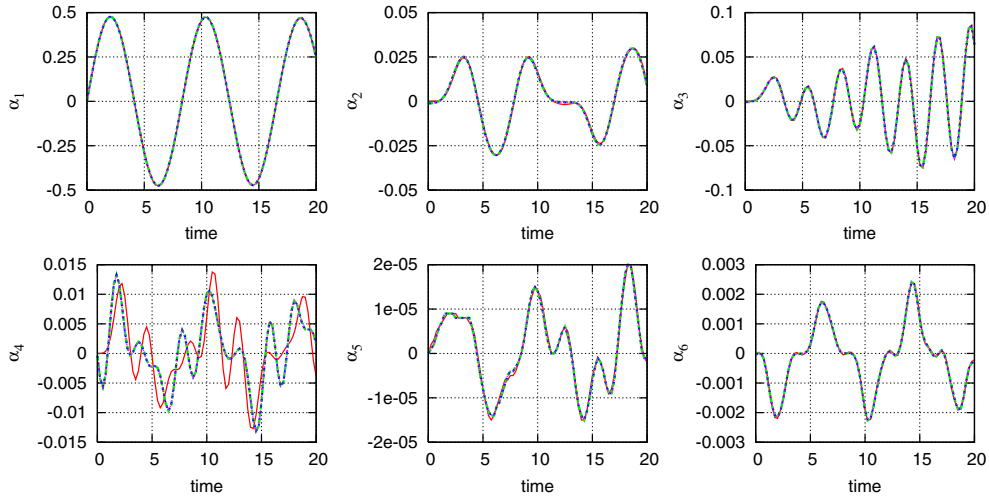

Figure 13. Short time evolution of $\alpha_i(t)$ for $i = 1-6$ from top left to bottom right. The same time evolutions for $t = kt_{\text{rec}}$ where $t_{\text{rec}} = 290$ and $k = 1-4$ are plotted on the same panels showing recurrence. The initial velocity is 0.5 and the system is started in the mode 1.

We conclude this section with an observation of recurrence similar to what happens for the Fermi–Pasta–Ulam system. Figure 13 presents a short time evolution of the first six modes for an initial velocity of 0.5, starting from the first mode. In the plots of figure 13 are superposed four other time evolutions taken at times $t = kt_{\text{rec}}$ where $t_{\text{rec}} = 290$ and k is an integer. This recurrence could indicate that our system is close to being integrable.

7. Conclusion

We considered the interaction between an electromagnetic field in a cavity and a thin polarized dielectric film. The model is the Maxwell–Lorenz system where the medium is described by

an oscillator and the coupling to the wave equation is through a Dirac delta function. We introduced normal modes which are adapted to the system film/cavity. These are well adapted to describe the time evolution of the system, unlike the standard sine Fourier modes or other Sturm–Liouville modes. The normal modes composed of the field E and the displacement Q are orthogonal with respect to a special scalar product which we introduce. The amplitude equations derived from the normal modes give an excellent description of the dynamics and could even be used as a numerical tool instead of solving the full partial differential equation system using the fairly involved finite volume method.

Assuming a linear oscillator for the film, we show conversion from one normal mode to another by forcing the film at specific frequencies. This is new for linear systems and could be used for many applications in optics or microwaves.

If the film is described by an anharmonic oscillator, the evolution generates other modes. Again the amplitude equations provide excellent agreement with the solution of the full problem. Finally we observed recurrence for certain initial velocities of the film. This phenomenon is known to exist for systems close to integrability. The fact that we observe it here may indicate that our system is in some ways close to integrability.

Acknowledgments

The authors thank André Draux and Yuri Gaididei for very useful discussions. Elena Kazantseva thanks the Region Haute-Normandie for a Post-doctoral grant. Andrei Maimistov is grateful to the *Laboratoire de Mathématiques, INSA de Rouen* for hospitality and support. The authors thank the Centre de Resources Informatiques de Haute-Normandie for access to computing resources.

Appendix A. Inconsistent projection using standard eigenmodes

Using standard Sturm–Liouville eigenmodes and the usual scalar product leads to inconsistent results. To show this let us assume no forcing for simplicity. We consider the usual eigenmodes associated with the Sturm–Liouville problem

$$E_{xx} - \alpha^2 E\delta(x - x_a) = -\omega^2 E. \tag{A.1}$$

Call these modes E_n associated with the eigenfrequency ω_n.

One then expands the field as

$$e(x,t) = \sum_{n=1}^{\infty} \alpha_n(t) E_n(x). \tag{A.2}$$

Plugging this expansion into the system of equations (10) and projecting onto the E_n using the standard scalar product, one gets the evolution of α's

$$\ddot{\alpha}_1 + \omega_1^2 \alpha_1 = \alpha\omega_0^2 q E_1(a), \tag{A.3}$$

$$\ddot{\alpha}_2 + \omega_2^2 \alpha_2 = \alpha\omega_0^2 q E_2(a), \tag{A.4}$$

$$\ddot{q} + \omega_0^2 q = \alpha \sum \alpha_i E_i(a). \tag{A.5}$$

Let us examine the jump condition on E_x from the partial differential equation (10). We have

$$-[E_x]_{x_a^-}^{x_a^+} = -\alpha\left[-\omega_0^2 q + \alpha E(a)\right]. \tag{A.6}$$

From expansion (A.2), we obtain

$$-[E_x]_{x_a^-}^{x_a^+} = -\sum_n \alpha_n [E_{nx}]_{x_a^-}^{x_a^+}.$$

We get the jumps of E_{nx} from the eigenvalue relation

$$E_{nxx} - \alpha^2 E_n \delta(x - x_a) = -\omega^2 E_n,$$

and obtain that

$$-\sum_n \alpha_n [E_{nx}]_{x_a^-}^{x_a^+} = -\alpha^2 \sum_n \alpha_n E_n(a) = -\alpha^2 E(a),$$

which is clearly inconsistent with the result obtained from the original system (A.6). Therefore one needs to use the normal modes associated with the full system and the special scalar product (37) to get a consistent reduced description of the system.

Appendix B. Numerical method for solving (10)

The evolution equation (10) involves a partial differential equation with a Dirac distribution coupled to an ordinary differential equation. We solve this coupled system using the method of lines where the time operator is kept as such and the space operator is discretized, naturally leading to a system of coupled ordinary differential equations. The spatial operator is a distribution so the natural way to give it meaning is to integrate it over small reference intervals (finite volume approximation). The value of the function is assumed to be constant in each volume. This method of lines allows us to increase the precision of the approximation in time and space independently.

We transform (10) into a system of first order partial differential equations

$$e_t = f, \tag{B.1}$$

$$f_t = e_{xx} - \alpha\delta(x - x_a) r_t, \tag{B.2}$$

$$q_t = r, \tag{B.3}$$

$$r_t = -\omega_0^2 q + \alpha e(x_a). \tag{B.4}$$

We then define our volume elements making sure that x_a is the center of one element. We then integrate the operator on each volume $[x_n - h/2, x_n + h/2]$ where h is the space step. For $x_n \neq x_a$, we recover the standard finite difference expression for the Laplacian

$$e_{xx} = \frac{e_{n+1} + e_{n+1} - 2e_n}{h^2} + O(h^2),$$

and get the discrete wave equation

$$\dot{e}_n = f_n, \tag{B.5}$$

$$\dot{f}_n = \frac{e_{n+1} + e_{n+1} - 2e_n}{h^2}. \tag{B.6}$$

For $x_n = x_a$, we get

$$\dot{e}_n = f_n, \tag{B.7}$$

$$\dot{f}_n = \frac{e_{n+1} + e_{n+1} - 2e_n}{h^2} - \alpha\dot{r}, \tag{B.8}$$

$$\dot{q} = r, \tag{B.9}$$

$$\dot{r} = -\omega_0^2 q + \alpha e_n. \tag{B.10}$$

The coupled system (B.5) and (B.7) is then integrated using an ordinary differential equation solver. In practice we use the variable step Runge–Kutta 4–5 Dopri5 developed by Hairer and Norsett at the University of Geneva [35].

References

[1] Newell A C and Moloney J V 1992 *Nonlinear Optics* (Reading, MA: Addison-Wesley)
[2] Walther H, Varcoe B T H, Englert B-G and Becker Th 2006 *Rep. Prog. Phys.* **69** 1325–82
[3] Vasilic B, Ott E, Antonen T, Barbara P and Lobb C J 2003 *Phys. Rev.* B **68** 024251
[4] Caputo J G and Loukitch L 2007 *Eur. Phys. J. Special Topics* **147** 95–112
[5] Horak P, Hechenblaikner G, Gheri K M, Stecher H and Ritsch H 1997 *Phys. Rev. Lett.* **79** 4974
[6] Shen J T and Fan S 2005 *Phys. Rev. Lett.* **95** 213001
[7] Rupasov V I and Yudson V I 1982 *Sov. J. Quantum Electron.* **12** 415
[8] Rupasov V I and Yudson V I 1987 *Sov. Phys.—JETP* **66** 282
[9] Ben-Aryeh Y, Bowden C M and Englund J C 1986 *Phys. Rev.* A **34** 3917–26
[10] Benedict M G, Zaitsev A I, Malyshev V A and Trifonov E D 1989 *Opt. Spectrosk.* **66** 726–8
[11] Benedict M G, Malyshev V A, Trifonov E D and Zaitsev A I 1991 *Phys. Rev.* A **43** 3845
[12] Elyutin S O and Maimistov A I 2001 *Opt. Spectrosk.* **90** 849–57
[13] Basharov A M, Maimistov A I and Elyutin S O 1999 *Zh. Eksp. Teor. Fiz.* **115** 30–42
[14] Elyutin S O and Maimistov A I 1999 *J. Mod. Opt.* **46** 1801–16
[15] Elyutin S O 2007 *Phys. Rev.* A **75** 023412
[16] Elyutin S O 2007 *J. Phys. B: At. Mol. Opt. Phys.* **40** 2533–50
[17] Malyshev V A, Ryzhov I V, Trifonov E D and Zaitsev A I 2000 *Opt. Commun.* **180** 59–68
[18] Benedict M G and Trifonov E D 1988 *Phys. Rev.* A **38** 2854–62
[19] Samson A M, Logvin Yu A and Turovets S I 1990 *Opt. Commun.* **78** 208–12
[20] Walther H, Varcoe B T H, Englert B-G and Becker T 2006 *Rep. Prog. Phys.* **69** 1325–82
[21] Caputo J-G, Kazantseva E V and Maimistov A I 2007 *Phys. Rev.* B **75** 14113
[22] Maimistov A I and Gabitov I R 2007 *Eur. Phys. J. Special Topics* **147** 265–86
[23] Meiser D and Meystre P 2006 *Phys. Rev.* A **74** 065801
[24] Bhattacharya M and Meystre P 2008 *Phys. Rev.* A **78** 041801
[25] Asboth J K, Ritsch H and Domokos P 2008 *Phys. Rev.* A **77** 063424
[26] Guedes I, Penaforte J C and Baseia B 1989 *Phys. Rev.* A **40** 2643
[27] Guea-Banacloche J, Lu N, Pedrotti L M, Prasad S, Scully M O and Wodkiewicz K 1990 *Phys. Rev.* A **41** 369
[28] Hildebrand R 1976 *Advanced Calculus for Applications* (Englewood Cliffs, NJ: Prentice-Hall)
[29] Courant R and Hilbert D 1959 *Methods of Mathematical Physics* (New York: Wiley)
[30] Dong H, Gong Z R, Ian H, Lan Zhou and Sun C P 2008 Intrinsic cavity qed and emergent quasi-normal modes for single photon arXiv:0805.3085v2 [quant-ph]
[31] Bocchieri P, Crotti A and Loinger A 1972 A classical solvable model of a radiant cavity *Lett. Nuovo Cimento* **4** 741–4
[32] Carslaw H S 1950 *An Introduction to the Theory of Fourier's Series and Integrals* (New York: Dover)
[33] Landau L and Lifchitz E 1969 *Mécanique* (Moscow: Mir)
[34] Scott A C (ed) 2005 *Encyclopedia of Nonlinear Science* (London: Taylor and Francis)
[35] Hairer E, Norsett S P and Wanner G 1987 *Solving Ordinary Differential Equations I* (Berlin: Springer)